HHS Public Access

Author manuscript

J Mater Chem B. Author manuscript; available in PMC 2020 July 07.

Published in final edited form as:

J Mater Chem B. 2019 July 7; 7(25): 3982–3992. doi:10.1039/c9tb00444k.

Mechanism of formation governs the mechanism of release of antibiotics from calcium phosphate nanopowders and cements in a drug-dependent manner

Vuk Uskoković

Department of Bioengineering, University of Illinois, Chicago, IL, USA.

Abstract

The kinetics of drug release from hydroxyapatite (HAp) cements could be tuned by controlling the kinetics of crystallization of their HAp precursor powders during synthesis. Here it is shown that this history of formation affects not only the kinetics, but also the mechanism of release. Cements composed of two HAp powders precipitated under different conditions, one (HAp2) taking twice longer to transform from the amorphous to the crystalline state than the other (HAp1), were mixed at different ratios to tune their drug release kinetics and tested for the release mechanism in conjunction with compositional and microstructural analyses. While the cement component converting to the amorphous phase during gelation (HAp2) exhibited a faster, but also more anomalous, non-Fickian mechanism of release of vancomycin, the cement component retaining its crystalline state all throughout gelation, setting and hardening (HAp1) stabilized at the ideal, Fickian diffusion case corresponding to the Korsmeyer–Peppas exponent value of 0.45 ± 0.02. This effect got reversed for the other antibiotic studied as a drug, ciprofloxacin, in which case HAp2 exhibited the ideal, Fickian diffusion with $n = 0.45 \pm 0.02$ and the increase in the content of the cement component retaining its crystallinity during gelation, setting and hardening (HAp1) steadily shifted the mechanism of release to more anomalous, non-Fickian types. This has indicated that the molecular structure of the drug is an essential determinant of the mechanism of release and that the design of a carrier for a universally tunable release of drugs based on the passive transport is likely impossible. Preliminary assays involving the addition of chitosan or gelatin as polymeric components to HAp led to the inclusion of swelling and erosion as additional effects by which the drug escapes the carrier and shifted the release toward less diffusional and more multimodal mechanisms. With regard to the microstructural and compositional effects governing the release mechanism and kinetics, the retention of a finite concentration of slit-like pores of the amorphous precursor in HAp2 and its lower surface energy and lesser drug binding potential in the gelled, amorphous state, but also its possibly less stable and more diffusive particle surface and higher structural water content were elaborated as potential reasons explaining the distinct rates and mechanisms of release from the two HAp powders with different histories of formation.

vuk21@yahoo.com.

Conflicts of interest

There are no conflicts to declare.

1. Introduction

Bone is a rarely versatile organ from structural and metabolic points of view. Its degree of heterogeneity, anisotropy and structural hierarchy is unusually high and has steadily disobeyed even the most ambitious attempts to synthetically replicate it. To illustrates its heterogeneity, it suffices to note that its structure gets denser and tissue turnover rate lower as one moves from its marrow cavity to the cancellous regions and then to the cortical outer layers. This variability in composition, structure and function presents a challenge for bone replacement therapies. What is more, these therapies often include the surgical placement of bone grafts that release specific therapeutic agents at sustained rates. Such agents may include an antibiotic for prophylactic purposes, to prevent bone infection due to inadvertently introduced pathogens, but also to treat an ongoing infection.[1] They may also include a bone morphogenetic protein to promote new bone growth,[2] an angiogenic factor to enhance neovascularization,[3] an anti-inflammatory drug to cope with the first stages of postoperative wound healing[4] or an immunosuppressant to prevent the immune rejection of implants such as allografts, xenografts or some synthetic materials.[5] However, the broad range of metabolic and turnover rates found in bone provides the bone therapists with a challenge of adjusting the rate of release of these compounds to the rate of their clearance from the tissues. For example, a drug release rate that proves itself optimal in trabecular bone may be misadjusted for the compact bone, and vice versa. Therefore, the task of providing clinicians with formulations whose drug release kinetics is adjustable *in situ* to the metabolism of not only each of the 206 bones in the body, but also to each particular region in each of these bones, is an ongoing one.

The demands for one such bone replacement material with *in situ* tunable drug release profiles necessitate the search for particular physicochemical parameters that can be used as “knobs” for adjusting these release rates.[6] Changes in chemistry are not always encouraged because of the potentially significant changes in the material properties induced thereby, causing not always desirable physiological effects. For example, lowering the cross-linking degree in a polymeric implant to create a looser structure and enable a quicker release of the drug from the formulation may increase the resorption rate of the implant and flood the tissue with the eroded particles or monomers whose presence above a specific concentration may trigger an inflammatory or toxic response. The physical parameters used before with limited success include the particle size,[7] crystallinity,[8] porosity,[9] the dopant concentration[10] and the particle shell-to-core volume ratio.[11] An earlier study demonstrated that the kinetics of the formation of a material can be controlled to produce drug release profiles tunable *in situ* to anywhere between 1 hour and 2 weeks of total release.[12] Specifically, mixing two differently synthesized hydroxyapatite (HAp) powders with a seemingly identical crystallinity and microstructure in different ratios allowed for the in situ adjustment of the rate of release of different antibiotics. This was the first report indicating that the mechanism of the formation of a solid compound can be used as a parameter to control the drug release kinetics in a strictly tunable manner. This effect was later tied to the presence of a memory effect in this particular material, HAp. Namely, specific structural features of the material retain traces of the pathways of their formation and continue to exhibit them at multiple levels, including physicochemical, but also biological.[13] It is not so often that history gets

inscribed in the present properties of a material, let alone that this history can be varied within such a range that it allows for tuning other properties within equally broad windows of values. Examples do exist, but are usually tied to the effect of the crystal growth conditions in the past on the growth rates in the future[14] and have not been utilized as control parameters for tuning other, more practical properties of interest. The question that this study wished to answer was if there was any difference in the mechanism of release between the formulations releasing the drugs at different rates thanks to the different kinetics of their formation mechanisms. Namely, per the study on which this work is based,[12] it is known that the mechanism of formation governs the release rates. However, does this difference in the mechanism of formation also imply a difference in the mechanism of the drug release across the range within which the release rates are tunable? In the attempt to answer this question, the release profiles of different formulations were fitted to a kinetic model that yields information about the release mechanism. At the same time, the analyses of microstructure, phase composition, crystallinity, specific surface area and porosity were conducted to get closer to the effects mechanistically governing the release of drugs from these formulations dependent on the history of formation of their two basic ingredients.

2. Materials and methods

2.1. Synthesis of drug-loaded calcium phosphate cements

Two different hydroxyapatite (HAp) powders – HAp1 and HAp2 – were synthesized. To make HAp1, 400 ml of 0.06 M aqueous solution of $NH_4H_2PO_4$ containing 25 ml 28% NH_4OH was added dropwise to the same volume of 0.1 M aqueous solution of $Ca(NO_3)_2$ (Fisher Scientific) containing 50 ml 28% NH_4OH (Sigma Aldrich), vigorously stirred with a magnetic bar (400 rpm) and kept on a plate heated to 50°C. After the addition of $NH_4H_2PO_4$ (Fisher Scientific) was complete, the suspension was brought to boiling, then immediately removed from the heater and air cooled to room temperature. Stirring was suspended and the precipitate together with its parent solution, the final pH of which was 10.6, were left to age in atmospheric conditions for 24 h. After the given time, the precipitate was washed once with deionized (DI) H_2O, centrifuged (10 s at 3500 rpm), and let dry overnight in a vacuum oven (Accu Temp-19, Across International) (p = −20 mmHg) at 80°C.

HAp2 was formed by abruptly adding a solution containing 100 ml 0.5 M $Ca(NO_3)_2$ and 7 ml 28% NH_4OH into a solution comprising 100 ml 0.2 M $NH_4H_2PO_4$ and 4 ml 28% NH_4OH. The fine precipitate formed upon mixing was aged for 15 s, then centrifuged, washed with 0.14 w/v% NH_4OH, centrifuged again, and dried overnight at low pressure (p = −20 mmHg) and room temperature. The pH of the supernatant following the precipitation reaction was 9.3. By washing the precipitate with ethanol or acetone and subsequently drying it at low pressure and storing at 4°C, it is possible to quench the composition in the amorphous form. However, for the purpose of this study, the powder was washed with water and allowed to spontaneously transform to HAp (*e.g.*, HAp2) at room temperature before being used in cement formation and release experiments.

The self-setting cements consisted of a solid and a liquid phase. The solid phase comprised either pure HAp1 and HAp2 powders or HAp1 and HAp2 powders mixed in different weight ratios (85/15 and 50/50). The liquid phase consisted of 2 wt% aqueous solution of

NaH_2PO_4. To load the cements with the drugs, either vancomycin (M.P. Biomedicals) or ciprofloxacin (Acros Organics) were added to the powder mixture in a 50 ml Falcon tube. This was followed by mixing using a digital vortex mixer (Fisher Scientific) for 5 min at 2000 rpm, after which 2 wt% Na_2HPO_4 (aq.) (Sigma Aldrich) was added dropwise to the solid mixture. Following this addition, the cement was again vortex mixed for 5 min at 2000 rpm. A constant solid-to-liquid ratio of 1.782 g ml^{-1} was employed, while the amount of the drug in each sample equaled 2.5 wt%. Table 1 shows the composition of the solid phase of the samples.

2.2. Microstructural and morphological characterization

Scanning Electron Microscopy (SEM) studies were carried out on a JEOL JSM 6320F-FESEM operated at 4.2 kV voltage and 8 mA beam current. Sample preparation involved depositing powders or pastes on clean aluminum stubs using the carbon tape and subsequently sputter-coating them with gold to reduce the charging effects. X-Ray Diffraction (XRD) was carried out on a Bruker D2 Phaser diffractometer using polychromatic Cu as the irradiation source. K_β line was stripped off with an inbuilt filter, whereas $K_{\alpha 2}$ line was stripped off manually. The step size was 0.01°, with 1 s of sample irradiation per step. Transmission electron microscopy (TEM) studies were performed on a JEOL JEM 1220 Life Science TEM operated at 80 kV.

2.3. *In vitro* drug release

The drug-loaded cements were allowed to completely set in a cylindrical form before they were placed in 50 ml of phosphate buffered saline (PBS) in closed conical tubes and incubated at 37°C and 50 rpm rotation perpendicular to the cylinder axis. The drug release rates from bone cements were determined by taking 1 ml PBS after 0.167 h (10 min), 0.5 h, 1 h, 2 h, 3 h, 4 h, 24 h and once every following day until 100% of the drug was released. The volume of the aliquoted solution was replaced each time with fresh PBS. The drug content was determined by measuring the corresponding absorbance on a UV/Vis spectrophotometer (Nanodrop 2000, ThermoScientific) at λ = 200 nm for vancomycin-containing samples and λ = 270 nm for ciprofloxacin-containing samples. Drug release profiles in the 0–60% release range were fitted to the Korsmeyer–Peppas equation in the following form, where M_t is the amount of the drug released by the time t, M_0 is the total amount of the drug entrapped in the carrier, k_m is the release rate constant calculated from the y-axis intercept and n is the Korsmeyer–Peppas exponent calculated from the slope and being indicative of the mechanism of the release:

$$\log\left(M_t/M_0\right) = \log k_{\mathrm{m}} + n\log t$$

The Korsmeyer–Peppas is one of many mathematical models used to fit the drug release curves and is presented here because of the highest goodness of the fit it produced in comparison to other similar models.[15] All data points in diagrams of drug release from pure HAp cements represent experimental duplicates (n = 2), while error bars represent standard deviation $\left(\mathrm{SD} = \left(\sum (x - \bar{x})^2/n\right)^{1/2}\right)$, the relatively low values of which indicate the appropriateness of the use of this number of experimental replicates. Duplicates are often

used in drug release assays in inorganic media[16–18] because of the abiological nature of these analyses, making them less of the subject of variability in the outcome compared to their biological analogues. All data points in diagrams of drug release from HAp/polymer composites represent experimental triplicates, while error bars represent standard deviation.

3. Results and discussion

A number of properties of HAp justify its use as a drug delivery agent, and they include: (i) exceptional biocompatibility and bioactivity; (ii) excellent sorption capacity, (iii) the ability to bind both negatively and positively charged drugs through electrostatic interaction with Ca^{2+} and PO_4^{3-} ions, respectively, and also engage in hydrogen bonding mediated by the OH^- group; (iv) sparse solubility (~0.3 μg ml^{-1}) and relatively long biodegradation times, which facilitate diffusion-controlled drug release kinetics; (v) the capability to capture drugs inside micropores formed within ultrafine particle aggregates, thus preventing the burst release and ensuring sustained release profiles; (vi) the propensity for accommodation of foreign ions that endow HAp with a range of electrical, magnetic, mechanical and optical properties not found in the pure compound, and others.[19,20] However, despite the fact that the first studies on HAp as a drug delivery carrier were done more than 30 years ago,[21–23] in the 1980s, meager progress has been made in the direction of allowing the release profiles in pure HAp ceramics to be tuned using sets of easily controllable structural parameters. It is hoped that a deeper understanding of the mechanism of release of drugs from HAp may bring the scientific community closer to the accomplishment of this vital practical goal. This hope has served as a motivation for this study.

At its onset, two different HAp powders were synthesized by precipitation from aqueous solutions and it was shown that they displayed highly similar particle sizes and morphologies. Specifically, as shown in Fig. 1a and d, both powders were monodisperse and composed of uniform nanoparticles with o100 nm in size. The nanoparticles were moderately agglomerated and this agglomeration naturally became more pronounced following the formation and setting of their cements (Fig. 1b and e). Although both powders displayed a similar, relatively poor crystallinity, their initial precipitates were amorphous and the timescale of their transformation to the crystalline phase differed: while HAp1 crystallized after 60–90 min of aging in the parent solution (Fig. 1c), HAp2 required 150–180 min to crystallize (Fig. 1f). Upon crystallization, the two materials displayed practically indistinguishable XRD patterns and the phase transformation appeared abrupt, matching the induction period model established previously for the precipitation of HAp from aqueous solutions.[24] According to this model, the amorphous system undergoes a series of subtle structural changes during the induction period, which are yet to be experimentally elucidated and which may last anywhere between minutes and days depending on supersaturation and the identity of foreign ions and surfaces in contact with the amorphous phase. These changes serve a preparatory purpose and culminate in a rather rapid phase transformation, thanks to which no intermediates between the amorphous and crystalline structures shown in Fig. 1c and f were detectable.

The rate of transition of reactants to products is normally inversely proportional to the extent of retention of reactants in the product. This implies that the probability that a process

catalyzing the reverse reaction will succeed in the reversal of the product to the reactants is higher in systems taking longer periods of time to react. This elementary kinetic effect explains why the propensity for the temporary return of these two crystalline powders to the amorphous state was markedly more pronounced in HAp2, the powder that spent more time in this intermediate amorphous state during synthesis and that it took longer to transform to HAp. Thus, while HAp2 fully transitioned to amorphous calcium phosphate (ACP) upon gelation and recrystallized upon hardening, no such transition was detected in HAp1 (Fig. 2). This transition was triggered by the contact with the mildly acidic solution of NaH_2PO_4 (pH ~ 6), which was used as the liquid for gelling the powders during the cement formation stage. The timescale of setting, hardening and reverting to the crystalline state depended on the sample volume, but was typically twice longer for HAp2 than for HAp1. Technically, therefore, HAp2 in the cement form could be treated as ACP, whereas HAp1 could be treated as HAp. At the same time, it should be kept in mind that this division is approximate, given that ACP invariably contains crystalline pockets and that HAp is poorly crystalline, meaning that the line dividing these two forms of calcium phosphate is blurred and not easy to draw.

Here it should be noted that the ability to vary the timescale of crystallization of HAp by controlling the reactant concentrations and the rate of their mixing is the consequence of the relatively low crystal growth rate even at very high nucleation rates, an antagonistic combination that is typical for this compound.[25] These low crystal growth and maturation rates are partially caused by the non-classical growth regimen dominated by the aggregation and coalescence of ultrafine particulates rather than by diffusion of ionic growth units.[26] Thanks to this combination of high nucleation rate and low crystal growth rate, ACP can be produced by simple precipitation reactions at room temperature, without having to rely on melt atomization or quenching at extremely high cooling rates, as most other ceramic materials do.[27–29] The slow crystal growth is also responsible for the wide variety of HAp crystal growth habits and particle morphologies producible by natural[30] or synthetic[31] means.

Cements formed by mixing HAp1 and HAp2 powders in different weight ratios yielded distinct release profiles for both antibiotics tested as drugs in this study: vancomycin (Fig. 3a) and ciprofloxacin (Fig. 4a). The rate of release was highest from the pure HAp2 cement and the lowest from the pure HAp1 cement. Most interestingly, the release rate could be tuned by controlling the weight ratio between HAp1 and HAp2. Simply, the more HAp2 in the cement, the faster the release and *vice versa*. The distinctness of the individual release profiles here depended on the identity of the drug: whereas the release curves were more neatly separated for vancomycin (Fig. 3a), they were more clumped together for ciprofloxacin (Fig. 4a). Thus, while the four different cement compositions, namely HAp2, HAp1/HAp2 50/50, HAp1/HAp2 85/15 and HAp1, completed the release of vancomycin in 2–3 h, 7–8 days, 11–14 days and 14–15 days, respectively, they completed the release of ciprofloxacin in 2–3 days, 14–15 days, 15–16 days and 16–17 days, respectively. This difference has also indicated that ciprofloxacin binds to HAp stronger than vancomycin, an insight that may appear counterintuitive considering the molecular structure of the two compounds. Namely, vancomycin is more hydrophilic (log $P = -3.1$) and also more massive (M_w = 1449.3 Da) than ciprofloxacin (log $P = 0.3$, M_w = 331.3 Da) and must bind stronger

electrostatically to the multivalent Ca^{2+} and PO_4^{3-} groups on the particle surface and form a greater density of hydrogen bonds with the OH^- groups of HAp. However, the desorption of a molecule from the particle surface (note that drug loading in HAp proceeds strictly *via* physisorption and never *via* intercalation or other forms of lattice entrapment) can be better described from the point of view of the competing affinity of the medium, in this case water, for both the particle surface and the drug molecule. With a predominantly hydrophilic molecule, this displacement will proceed more effectively than with a predominantly hydrophobic one, explaining the faster release of vancomycin than that of ciprofloxacin.

The analysis of the Korsmeyer–Peppas fits showed that the mechanism of release of vancomycin was directly dependent on the mechanism of formation of the HAp cement. Namely, while the Korsmeyer–Peppas exponent, n, indicative of the release mechanism in the initial period of release was 0.68 ± 0.04 (r^2 = 0.993) for the fastest releasing, HAp2 formulation, it steadily dropped as the content of HAp1 in the cement increased: to0.61 ± 0.05 (r^2 = 0.974) for HAp1/HAp2 50/50 and 0.61 ± 0.02 (r^2 = 0.997) for HAp1/HAp2 85/15 to 0.54 0.02 (r^2 = 0.997) for pure HAp1 (Fig. 3b–f). Per the Korsmeyer–Peppas model, $n \sim 0.45$ for cylindrical samples signifies Fickian diffusion, $n < 0.45$ pseudo-Fickian diffusion, $0.45 < n < 0.89$ anomalous, non-Fickian diffusion, $0.89 < n < 1$ zero-order, non-Fickian case II relaxation and $n > 1$ non-Fickian super case II.[32] Therefore, in the case of vancomycin, a shift from the amorphous to the crystalline content in HAp results in the shift from the release *via* more anomalous, non-Fickian diffusion to the release *via* more regular, Fickian diffusion. Because of the aforementioned possibility of loading HAp strictly *via* drug adsorption, not encapsulation, the release is, expectedly, driven by diffusion, not dissolution of the carrier, as in the case of polymers, and this effect can be further confirmed by the absence of any considerable degradation of the cement during the period of release. Therefore, although $n > 0.45$ is often interpreted as the combination of diffusion and swelling/erosion, one such mechanism is not applicable to calcium phosphate cements. Despite the obvious hydration of the cement, the setting and hardening processes in cements in general are accompanied by shrinkage,[33] not swelling, even when they occur in liquid environments.[34]

Interestingly, while pure HAp2 cement exhibited a single mechanism throughout the entire, albeit short, only 2–3 h long period of release (Fig. 3b), the mechanism of release shifted in favor of the normal, Fickian diffusion and disfavor of the anomalous, non-Fickian diffusion at longer timescales, typically >10 h, for all cements containing HAp1 (Fig. 3c–e). Eventually, for the pure HAp1 cement, the release after 10 h steadied at $n = 0.45 \pm 0.02$ (r^2 = 0.992), the exact value corresponding to the ideal Fickian diffusion as the release mechanism, agreeing with the previous release kinetics studies on HAp powders and cements.[35–37] Finally, in the case of vancomycin, as the content of HAp1 in the cement increased, both the rate constant of the release, k_m, and the release exponent, n, decreased (Fig. 3f). Perhaps most interestingly, this effect of the cement content on the release exponent and the release mechanism was reversed in the case of ciprofloxacin, in which case the rate constant decreased as the content of HAp1 increased, but the Korsmeyer–Peppas exponent increased (Fig. 4f). Specifically, while the release exponent, n, in the total period of release was 0.45 ± 0.02 (r^2 = 0.987), signifying the ideal Fickian diffusion, for the fastest releasing, HAp2 formulation, it steadily increased with the content of HAp1 in the cement:

to 0.75 ± 0.04 (r^2 = 0.987) for HAp1/HAp2 50/50, 1.28 ± 0.07 (r^2 = 0.978) for HAp1/HAp2 85/15 and 1.86 ± 0.07 (r^2 = 0.988) for pure HAp1 (Fig. 4b–e). This diametrically opposite effect that the cement content has on the mechanism of release of vancomycin and ciprofloxacin is unexpected and difficult to explain. Also, unlike in the case of vancomycin, when all HAp1-containing formulations exhibited a bimodal release mechanism (Fig. 3c–e), the more anomalous, non-Fickian model applying to $t < 10$ h and the more classical, Fickian model applying to $t > 10$ h, all formulations exhibited a single mechanism of release of ciprofloxacin throughout the entire period of release, as demonstrated by the linear fits extending from the earliest to the final, ~60% release time points (Fig. 4b–e).

These results show that the mechanism of formation of a material comprising the drug delivery carrier, in this case HAp, can affect the mechanism of drug release in addition to affecting the drug release kinetics. Moreover, this mechanism of release is evidently dependent on the molecular structure of the drug. Not only does this physicochemical nature of the drug determine how tunable the release profiles will be (Fig. 3a and 4a), but they also, as it is demonstrated here, define the characteristics of the mechanism of release (Fig. 3f and 4f). This effect is logical because the release is, deep down, an interfacial process occurring through an interaction between the carrier and the drug. This observation shatters the illusion that the design of a carrier for the universally tunable release of drugs is possible. Rather, understanding the fundamentals of the drug/carrier interaction is necessary before the correspondence between the particular physical properties of the carrier and the release kinetics can be established.

In the attempt to decipher the possible microstructural effects responsible for this difference in the kinetics and mechanism of release from the two highly similar HAp powders, differing mostly in the formation pathway, the specific surface areas (S_a) and porosities of these two materials and of the ACP precursor of HAp2 were measured and the results are shown in Fig. 5. The pore size distribution of powders HAp1 and HAp2 was very similar, but not identical, with the only difference lying in the retention of the borderline micropore peak at 3.6 nm from the amorphous precursor in HAp2. Both distributions were broad and peaked in the mesoporous range, at 25.4 nm for HAp1 and 22.6 nm for HAp2. S_a of HAp2 was somewhat higher than that of HAp1, specifically 88.9 $m^2\ g^{-1}$ *vs.*76.2 $m^2\ g^{-1}$, and was highly similar, almost identical to that of the ACP precursor of HAp2, hinting at this retention of some microstructural properties of ACP by HAp2. The large difference in porosity between ACP and HAp2 in spite of the identical S_a values is explained by the presence of slit-like pores in ACP, which are narrow and composed of long “walls”, contributing to a relatively large S_a despite the low porosity. However, these slit-like pores collapse and convert to larger mesopores upon the transition to HAp2 and only a minor presence of theirs gets retained in the material, as evidenced by the 3.6 nm peak in HAp2. This bimodal distribution of pore sizes fits the non-Fickian model that applied to HAp2 during the release of vancomycin and that is defined by the existence of a sharp boundary between the more hydrated and the less hydrated regions in the carrier.[38] However, the fact that the same effect did not apply to HAp2 during the release of ciprofloxacin and that HAp1 in that case displayed more non-Fickian release patterns suggests that this bimodality does not play a crucial effect in defining the release mechanistically. HAp1 and HAp2 powders exhibited highly similar pore volumes of 0.61 $cm^3\ g^{-1}$ and 0.65 $cm^3\ g^{-1}$, respectively, and

this minimal difference in the pore size volume and distribution suggests that the difference in drug release profiles between HAp1 and HAp2 is neither caused by the difference in porosity. The fact that HAp2 had a lower average pore size, but released drugs considerably faster than HAp1 additionally indicates that porosity, which is often a critical determinant of the release kinetics,[39–41] has no significant role in controlling the rate of the drug release from HAp cements. Porosity reduction or expansion often entail the drug release process in HAp,[42] but in this case the pores alone cannot be the sole cause of the difference in drug release patterns. More probably, this difference must be explained by a difference at the particle surface level or, more specifically, at the triple junction between (i) the particle surface, (ii) water and (iii) the drug molecule. With HAp2 transitioning to ACP upon cement formation, albeit only to return to HAp upon setting, the HAp2 phase initially in contact with the drug could be treated as ACP, in contrast to HAp1, which retains HAp identity all throughout gelation, setting and hardening. The surface energy of ACP is lower than that of HAp because of both enthalpic and entropic reasons, the former being rooted in weaker bonds and the lower density of bonds on an amorphous surface and the latter being rooted in the greater similarity of the order of the amorphous phase to the inherently disordered liquid phase surrounding it. This surface energy argument implies that drug binding will be weaker and desorption faster from ACP than from HAp. This argument, however, is applicable only in the first hour of release because by the end of the first hour, ACP will have fully converted to HAp (Fig. 2b). Since the timescale of this crystallization (30 min for HAp1 and 60 min for HAp2 for 0.5 g cylinders) is lower than the timescale of the release (14–15 days for HAp1 and 2–3 h for HAp2), the difference in the surface energy between ACP and HAp cannot be the sole cause of the difference in the release rate. The higher degree of the constantly ongoing exchange of ionic units and clusters across the particle surface in contact with an aqueous solvent in ACP than in HAp may get retained in HAp2 and present another factor potentially at work. Yet another, possibly crucial effect is that of structural water. Per previous analyses,[43] ACP contains 24.6 wt% water compared to only 6.5 wt% in HAp and this water does get mostly retained in HAp2. This water may provide a key channel for the water from the solvent to enter the structure and wash away the drug content adhering to the particle surface. In this scenario, the structural water enables the solvent water to overcome its surface tension at the mesoporous grain interface and penetrate the pores that may otherwise be impenetrable in its absence, thus being potentially a key to explaining the faster release from HAp2 than from HAp1.

To test whether the release mechanism will change upon the addition of polymers to HAp powders and cements, HAp1 powder containing only 0.05 wt% of chitosan and HAp1 cement containing 20 wt% of gelatin were synthesized and tested for drug release profiles. TEM images are provided in Fig. 6, showing HAp nanoparticles separated in a powder form by thin interfacial layers of chitosan (Fig. 6a) or suspended in a matrix of gelatin (Fig. 6b). Interestingly, only 0.05 wt% of chitosan was sufficient to stabilize the drug adsorbed onto HAp and induce a significantly more sustained release compared to the monophasic HAp powder (Fig. 6c), where the drug was bound by comparatively weaker forces to the particle surface and desorbed more easily. The addition of 20 wt% of gelatin to HAp1 cement had an ever more drastic effect on delaying the release, as only 10% of vancomycin got released after 21 days of the release time (Fig. 6c), in contrast to the release of vancomycin being

completed in 15 days from pure HAp1 cement (Fig. 3a). The comparison of release mechanisms showed that $n = 0.68 \pm 0.04$ ($r^2 = 0.986$) for chitosan-supplemented HAp1 (Fig. 6d), indicating the anomalous mechanism, where some release occurs via swelling and erosion of the protective polymeric layers entrapping the drug in addition to the drug diffusing directly off the polymeric network and HAp particle surface. As for the gelatin-containing systems, n increased from the average of 0.50 ± 0.02 ($r^2 = 0.995$) for gelatin-free HAp1 cement to 1.00 ± 0.01 ($r^2 = 1.000$) for gelatin-containing HAp1 cement in the initial 100 h of the release time (Fig. 6e), suggesting the same coupling of swelling and erosion to the classical diffusion as that applying to chitosan-containing HAp1 as the mechanism of release. As the content of gelatin in the composite cements gets depleted, at $t > 100$ h, so does the release exponent decrease in value, eventually steadying at $n = 0.22 \pm 0.01$ ($r^2 = 0.993$) (Fig. 6e), suggesting the freeing of the HAp surface and the transition to more classical diffusion of the drug as the mechanism of its escape from the carrier. It is conceivable that this mechanism will be further modified at different contents of the polymeric phase(s) and that it may take different forms for different drugs loaded onto the HAp carrier. To answer these and other questions pertaining to the drug-dependency of the release mechanism from such composite carriers, more detailed kinetic analyses, involving a broader spectrum of variables, must be conducted. The preliminary tests performed here still unequivocally demonstrate that the addition of chitosan or gelatin as polymeric components to HAp gives rise to swelling and erosion as additional mechanisms of release and shifts the latter toward less diffusional and more multimodal types.

4. Conclusions

Controlled drug release achieved by controlling merely the history of formation of different HAp powders in a self-setting bone cement is an intriguing effect. To that end, two HAp powders precipitated under different conditions, one (HAp2) taking twice longer to transform from the amorphous to the crystalline state than the other (HAp1), could be mixed at different ratios to tune their drug release kinetics to the desired physiological scenario. Here it is shown that this history of formation affects not only the kinetics, but also the mechanism of release. Thus, while the cement component converting to the amorphous phase during gelation (HAp2) exhibited a faster, but also more anomalous, non-Fickian mechanism of release of vancomycin, the cement component retaining its crystalline state all throughout gelation, setting and hardening (HAp1) stabilized at the ideal, Fickian diffusion case corresponding to the Korsmeyer–Peppas exponent value of 0.45 ± 0.02. This effect, however, got reversed for the other antibiotic studied as a drug, ciprofloxacin, in which case HAp2 exhibited the ideal, Fickian diffusion with $n = 0.45 \pm 0.02$ and the increase in the content of the cement component retaining its crystallinity during gelation, setting and hardening (HAp1) steadily shifted the mechanism of release to more anomalous, non-Fickian types. This has indicated that the molecular structure of the drug is an essential determinant of the mechanism of release and that understanding the drug/carrier interaction is necessary before the exact correspondence between the physical properties of the carrier and the release kinetics can be established. The addition of chitosan or gelatin as polymeric components to HAp led to the inclusion of swelling and erosion as additional effects by which the drug escapes the carrier and shifted the release toward less diffusional and more

multimodal mechanisms. With regard to the microstructural and compositional effects governing the release mechanism and kinetics, the retention of a finite concentration of slit-like pores of the amorphous precursor in HAp2 and its lower surface energy and lesser drug binding potential in the gelled, amorphous state, but also its possibly less stable and more diffusive particle surface and higher structural water content were all studied and/or considered as potential reasons explaining the distinct rates and mechanisms of release from the two HAp powders with different histories of formation. This intriguing effect lying at the triple junction between the properties of the particle, the properties of the released molecule and the properties of the aqueous medium warrants further research into their synergies, with corollaries spilling from the sphere of basic physical chemistry to the realms of pharmacy, medicine and beyond.

Acknowledgements

The author acknowledges Shreya Ghosh and Maheshwar Iyer from the Uskoković Lab at the University of Illinois in Chicago for assistance with XRD, TEM and release measurements, Ivona Janković-Častvan from the University of Belgrade for assistance with porosity measurements, and the National Institutes of Health grant R00-DE021416 for the financial support.

References

1. Uskoković V, Nanostructured Platforms for the Sustained and Local Delivery of Antibiotics in the Treatment of Osteomyelitis, Crit. Rev. Ther. Drug Carrier Syst, 2015, 32(1), 1–59. [PubMed: 25746204]
2. Gonzaga MG, Dos Santos Kotake BG, de Figueiredo FAT,Feldman S, Ervolino E, Dos Santos MCG and Issa JPM, Effectiveness of rhBMP-2 association to autogenous, allogeneic, and heterologous bone grafts, Microsc. Res. Tech, 2019, 82(6), 689–695. [PubMed: 30637849]
3. Huang C, Das A, Barker D, Tholpady S, Wang T, Cui Q, Ogle R and Botchwey E, Local delivery of FTY720 accelerates cranial allograft incorporation and bone formation, Cell Tissue Res, 2012, 347(3), 553–566. [PubMed: 21863314]
4. Madhumathi K, Rubaiya Y, Doble M, Venkateswari R and Sampath Kumar TS, Antibacterial, anti-inflammatory, and bone-regenerative dual-drug-loaded calcium phosphate nanocarriers-*in vitro* and *in vivo* studies, Drug Delivery Transl. Res, 2018, 8(5), 1066–1077.
5. Sakakura CE, Margonar R, Sartori R, Morais JA and Marcantonio E Jr., The influence of cyclosporin a on mechanical retention of dental implants previously integrated to the bone: a study in rabbits, J. Periodontol, 2006, 77(12), 2059–2062. [PubMed: 17209791]
6. Uskoković V and Ghosh S, Carriers for the Tunable Release of Therapeutics: Etymological Classification and Examples, Expert Opin. Drug Delivery, 2016, 13(12), 1729–1741.
7. Zhang P, Gómez De La Torre TZ, Forsgren J, Bergström C and Strømme M, Diffusion-Controlled Drug Release from the Mesoporous Magnesium Carbonate Upsalite®, J. Pharm. Sci, 2015, 105(2), 657–663. [PubMed: 26087956]
8. Hamanishi C, Kitamoto K, Tanaka S, Otsuka M and Kitahashi T, A Self-setting TTCP-DCPD Apatite Cement for Release of Vancomycin, J. Biomed. Mater. Res, 1996, 33(3), 139–143. [PubMed: 8864885]
9. Hou H, Nieto A, Ma F, Freeman WR, Sailor MJ and Cheng L, Tunable Sustained Intravitreal Drug Delivery System for Daunorubicin Using Oxidized Porous Silicon, J. Controlled Release, 2014, 178, 46–54.
10. Lu D, Lei J, Wang L and Zhang J, Multifluorescently Traceable Nanoparticle by a Single-Wavelength Excitation with Color-Related Drug Release Performance, J. Am. Chem. Soc, 2012, 134(21), 8746–8749. [PubMed: 22591275]
11. Orellana BR and Puleo DA, Tailored Sequential Drug Release from Bilayered Calcium Sulfate Composites, Mater. Sci. Eng., C, 2014, 43, 243–252.

12. Ghosh S, Wu VM, Pernal S and Uskoković V, Self-Setting Calcium Phosphate Cements with Tunable Antibiotic Release Rates for Advanced Bone Graft Applications, ACS Appl. Mater. Interfaces, 2016, 8(12), 7691–7708. [PubMed: 26958867]
13. Uskoković V, Tang S and Wu VM, On Grounds of the Memory Effect in Amorphous and Crystalline Apatite: Kinetics of Crystallization and Biological Response, ACS Appl. Mater. Interfaces, 2018, 10(17), 14491–14508. [PubMed: 29625010]
14. Pantaraks P, Matsuoka M and Flood AE, Effect of Growth Rate History on Current Crystal Growth. 2. Crystal Growth of Sucrose, $Al(SO_4)_2$ $12H_2O$, KH_2PO_4, and K_2SO_4, Cryst. Growth Des, 2007, 7(12), 2635–2642.
15. Carbinatto FM, de Castro AD, Evangelista RC and Cury BSF, Insights into the swelling process and drug release mechanisms from cross-linked pectin/high amylose starch matrices, Asian J. Pharm. Sci, 2014, 9, 27–34.
16. Chorny M, Fishbein I, Danenberg HD and Golomb G, Lipophilic drug loaded nanospheres prepared by nano-precipitation: effect of formulation variables on size, drug recovery and release kinetics, J. Controlled Release, 2002, 83, 389–400.
17. Krasko MY, Golenser J, Nyska A, Nyska M, Brin YS and Domb AJ, Gentamicin extended release from an injectable polymeric implant, J. Controlled Release, 2007, 117, 90–96.
18. Caccavo D, Lamberti G, Barba AA, Abrahmsen-Alami S, Viridien A and Larsson A, Effects of HPMC substituent pattern on water up-take, polymer and drug release: An experimental and modelling study, Int. J. Pharm, 2017, 528, 705–713. [PubMed: 28636894]
19. Wu VM and Uskoković V, Waiting for Apatao: 250 Years Later, Found. Sci, 2019, DOI: 10.1007/s10699-019-09602-x.
20. Mondal S, Dorozhkin SV and Pal U, Recent progress on fabrication and drug delivery applications of nano-structured hydroxyapatite, Wiley Interdiscip. Rev.: Nanomed. Nanobiotechnol, 2018, 10, e1504. [PubMed: 29171173]
21. Eitenmüller J, Schmidt KH, Peters G, Gellissen G, Weltin R and Reichmann W, Experimental and preliminary clinical experience with absorbable calcium phosphate granules containing an antibiotic or antiseptic for the local treatment of osteomyelitis, J. Hosp. Infect, 1985, 6, 117–184. [PubMed: 2860155]
22. Kawamura M, Iwata H, Sato K and Miura T, Chondroosteogenic response to crude bone matrix proteins bound to hydroxyapatite, Clin. Orthop. Relat. Res, 1987, 217, 281–292.
23. Uchida A, Shinto Y, Araki N and Ono K, Development of a slow release system of anti-cancer drugs retained in calcium-hydroxyapatite ceramic, Gan to Kagaku Ryoho, 1989, 16, 3231–3235. [PubMed: 2551252]
24. Uskoković V, Li W and Habelitz S, Amelogenin as a Promoter of Nucleation and Crystal Growth of Apatite,J. Cryst. Growth, 2011, 316, 106–117.
25. Uskoković V, The Role of Hydroxyl Channel in Defining Selected Physicochemical Peculiarities Exhibited by Hydro-xyapatite, RSC Adv, 2015, 5, 36614–36633. [PubMed: 26229593]
26. Du LW, Bian S, Gou BD, Jiang Y, Huang J, Gao YX, Zhao YD, Wen W, Zhang TL and Wang K, Structure of clusters and formation of amorphous calcium phosphate and hydroxyapatite: from the perspective of coordination chemistry, Cryst. Growth Des, 2013, 13, 3103–3109.
27. Ciftci N, Ellendt N, Barreto ES, Madler L and Uhlenwinkel V, Increasing the amorphous yield of $\{(Fe_{0.6}Co_{0.4})(0.75)B_{0.2}\text{-}Si_{0.05}\}_{(96)}$Nb-4 powders by hot gas atomization, Adv. Powder Technol, 2018, 29, 380–385.
28. Pan JY, Zheng YT, Zheng YD, Ye W and Yu WJ, Solidification mechanism and microstructure evolution of Al_2O_3–ZrO_2 ceramic coating prepared by combustion synthesis and thermal explosion spraying, Ceram. Int, 2017, 43, 4037–4041.
29. Goel A, Ferrari AM, Kansal I, Pascual M. j., Barbieri L, Bondioli F, Lancellotti I, Ribeiro MJ and Ferreira JMF, Sintering and crystallization behavior of $CaMgSi_2O_6$–$NaFe\text{-}Si_2O_6$ based glass-ceramic, J. Appl. Phys, 2009, 106, 093502.
30. Daculsi G, Bouler J-M and LeGeros RZ, Adaptive crystal formation in normal and pathological calcifications in synthetic calcium phosphate and related biomaterials, Int. Rev. Cytol, 1997, 172, 129–191. [PubMed: 9102393]

31. Sadat-Shojai M, Khorasani MT, Dinpanah-Khoshdargi E and Jamshidi A, Synthesis methods for nanosized hydro-xyapatite with diverse structures, Acta Biomater, 2013, 9, 7591–7621. [PubMed: 23583646]
32. Ritger PL and Peppas NA, A simple equation for description of solute release II. Fickian and anomalous release from swellable devices, J. Controlled Release, 1987, 5, 37–42.
33. Acker P, Swelling, shrinkage and creep: a mechanical approach to cement hydration, Mater. Struct, 2004, 37, 237–243.
34. Bortolotto T, Guillarme D, Gutemberg D, Veuthey JL and Krejci I, Composite resin vs. resin cement for luting of indirect restorations: comparison of solubility and shrinkage behavior, Dent. Mater. J, 2013, 32(5), 834–838. [PubMed: 24088842]
35. Nayak AK, Hasnain MS and Malakar J, Development and optimization of hydroxyapatite-ofloxacin implants for possible bone delivery in osteomyelitis treatment, Curr. Drug Delivery, 2013, 10, 241–250.
36. Nayak AK, Laha B and Sen KK, Development of hydroxyapatite-ciprofloxacin bone-implants using ‘Quality by design’, Acta Pharm, 2011, 61, 25–36. [PubMed: 21406341]
37. Melville AJ, Rodríguez-Lorenzo LM and Forsythe JS, Effects of calcination temperature on the drug delivery behaviour of Ibuprofen from hydroxyapatite powders,J. Mater. Sci.: Mater. Med, 2008, 19(3), 1187–1195. [PubMed: 17701302]
38. Kee DD, Liu Q and Hinestroza J, Viscoelastic (Non-Fickian) Diffusion, Can. J. Chem. Eng, 2005, 83, 913–929.
39. Otsuka M, Nakahigashi Y, Matsuda Y, Kokubo T, Yoshihara S, Fujita H and Nakamura T, The in vitro and in vivo indomethacin release from self-setting bioactive glass bone cement, Biomed. Mater. Eng, 1997, 7(5), 291–302. [PubMed: 9457380]
40. Unagolla JM and Jayasuriya AC, Drug transport mechanisms and in vitro release kinetics of vancomycin encapsulated chitosan-alginate polyelectrolyte microparticles as a controlled drug delivery system, Eur. J. Pharm. Sci, 2018, 114, 199–209. [PubMed: 29269322]
41. Rahma A, Munir MM, Khairurrijal, Prasetyo A, Suendo V and Rachmawati H, Intermolecular Interactions and the Release Pattern of Electrospun Curcumin-Polyvinyl(pyrrolidone) Fiber, Biol. Pharm. Bull, 2016, 39(2), 163–173. [PubMed: 26830478]
42. Otsuka M, Nakahigashi Y, Matsuda Y, Fox JL and Higuchi WI, A novel skeletal drug delivery system using self-setting calcium phosphate cement. 7. Effect of biological factors on indomethacin release from the cement loaded on bovine bone, J. Pharm. Sci, 1994, 83, 1569–1573. [PubMed: 7891276]
43. Uskoković V, Marković S, Veselinović Lj., Ŝkapin S, Ignjatović N and Uskoković DP, Insights into the Kinetics of Thermally Induced Crystallization of Amorphous Calcium Phosphate, Phys. Chem. Chem. Phys, 2018, 20, 29221–29235. [PubMed: 30427330]

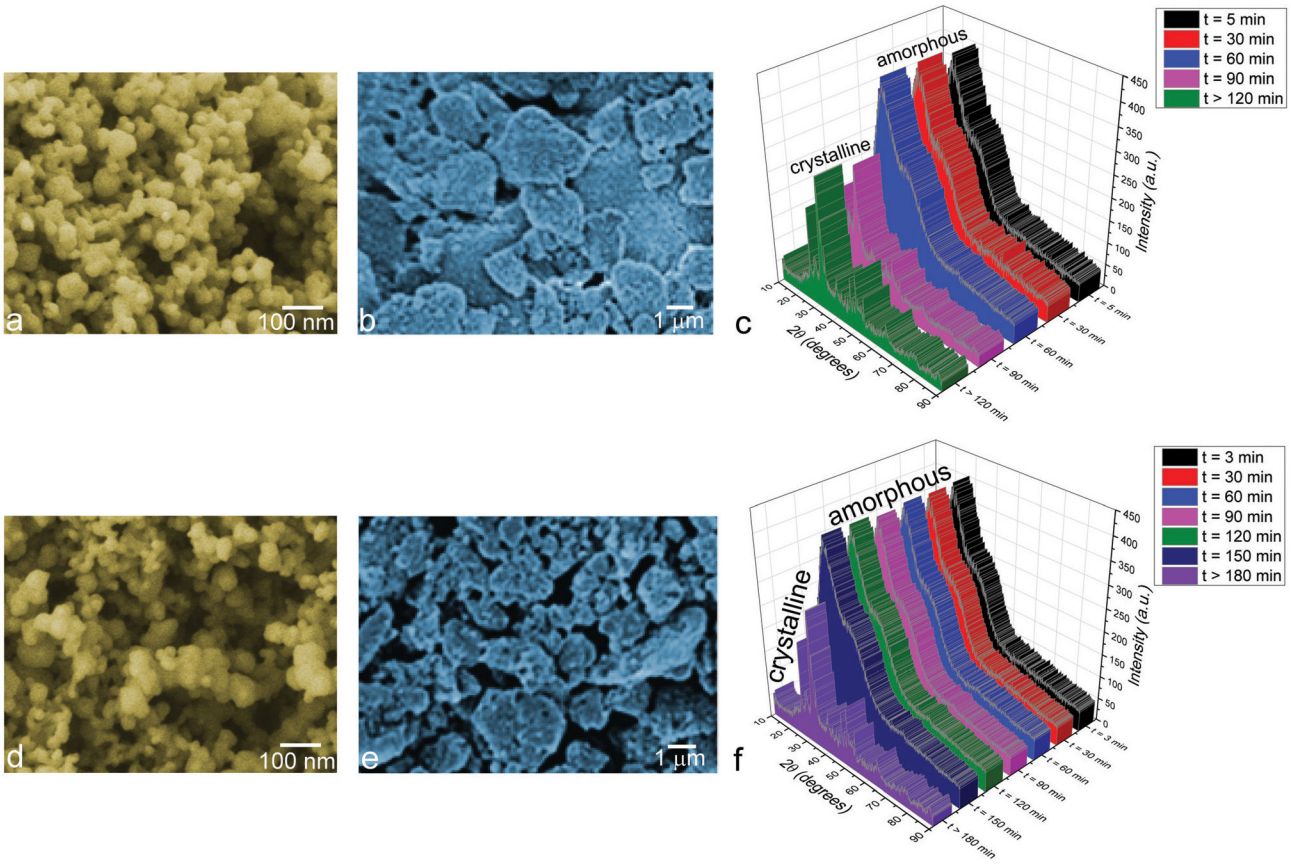

Fig. 1.

SEM images of HAp1 (a and b) and HAp2 (d and e) nanoparticles before (a and d) and after (b and e) the cement formation and setting, along with the XRD patterns showing their time-dependent transformation from an amorphous phase to HAp (HAp1 – c, HAp2 – f).

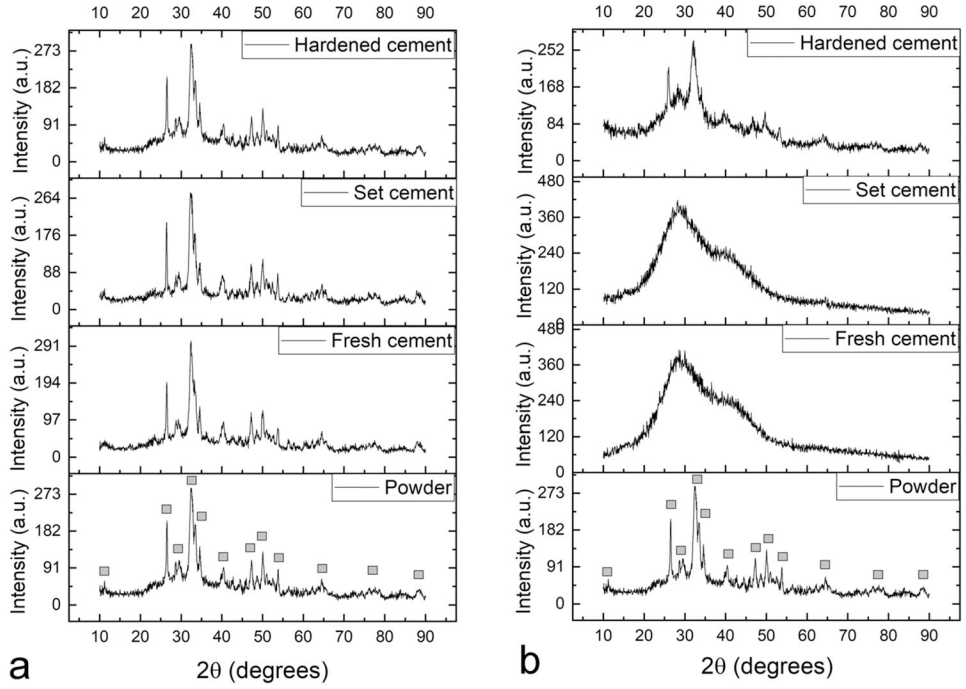

Fig. 2.

XRD patterns showing the evolution of crystallinity of HAp1 (a) and HAp2 (b) powders during the successive cement formation, setting and hardening stages. Diffraction peaks originating from HAp are labeled with gray squares and the diffuse diffractograms with broad reflections at low 2y in(b) signify amorphousness of the material.

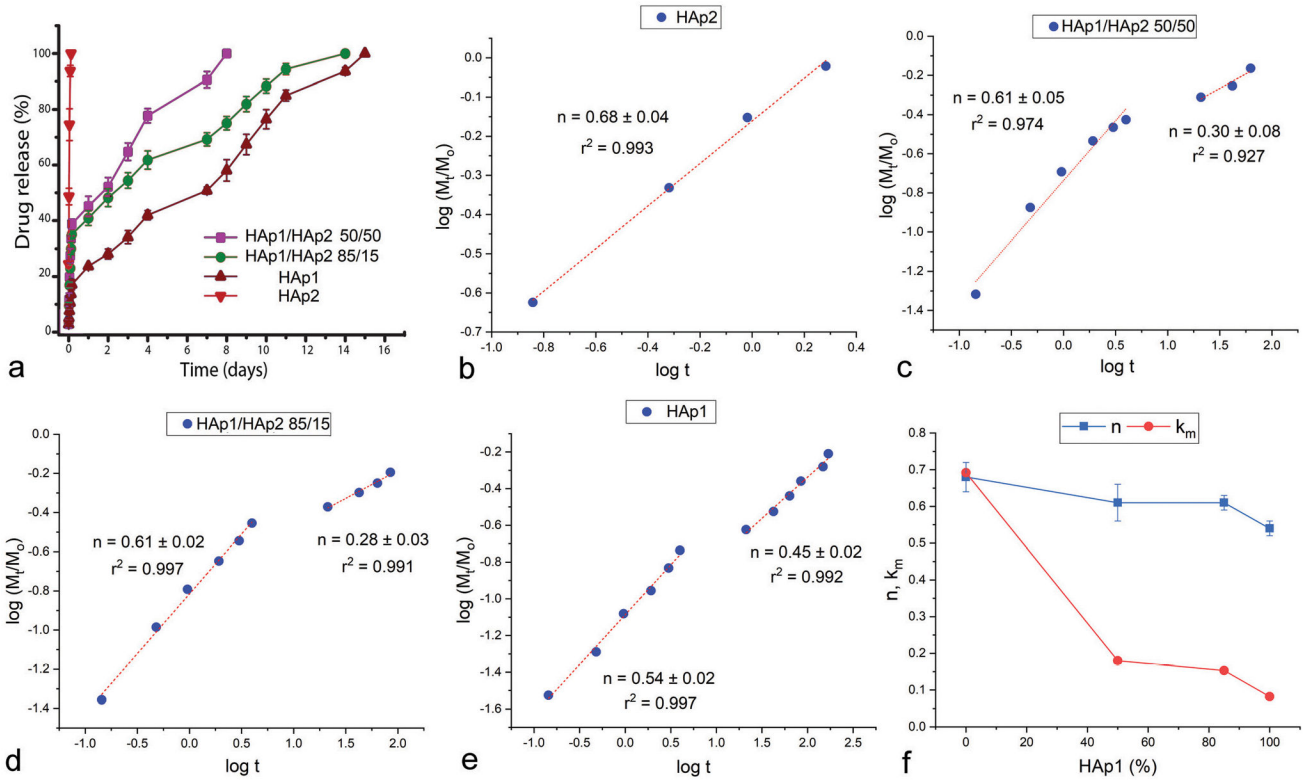

Fig. 3.

Vancomycin kinetic release profiles of cements composed of HAp1 and HAp2 alone and HAp1 and HAp2 mixed in 85/15 and 50/50 weight ratios (a). Linear fits of the release data for the four different cements, including HAp2 (b), HAp1/HAp2 50/50 (c), HAp1/HAp2 85/15 (d) and HAp1 (e), to the Korsmeyer–Peppas model, from which the Korsmeyer–Peppas exponent, n, was derived. Variation in the parameter n and the release rate constant, k_m, as a function of the content of HAp1 in the mixed cements (f).

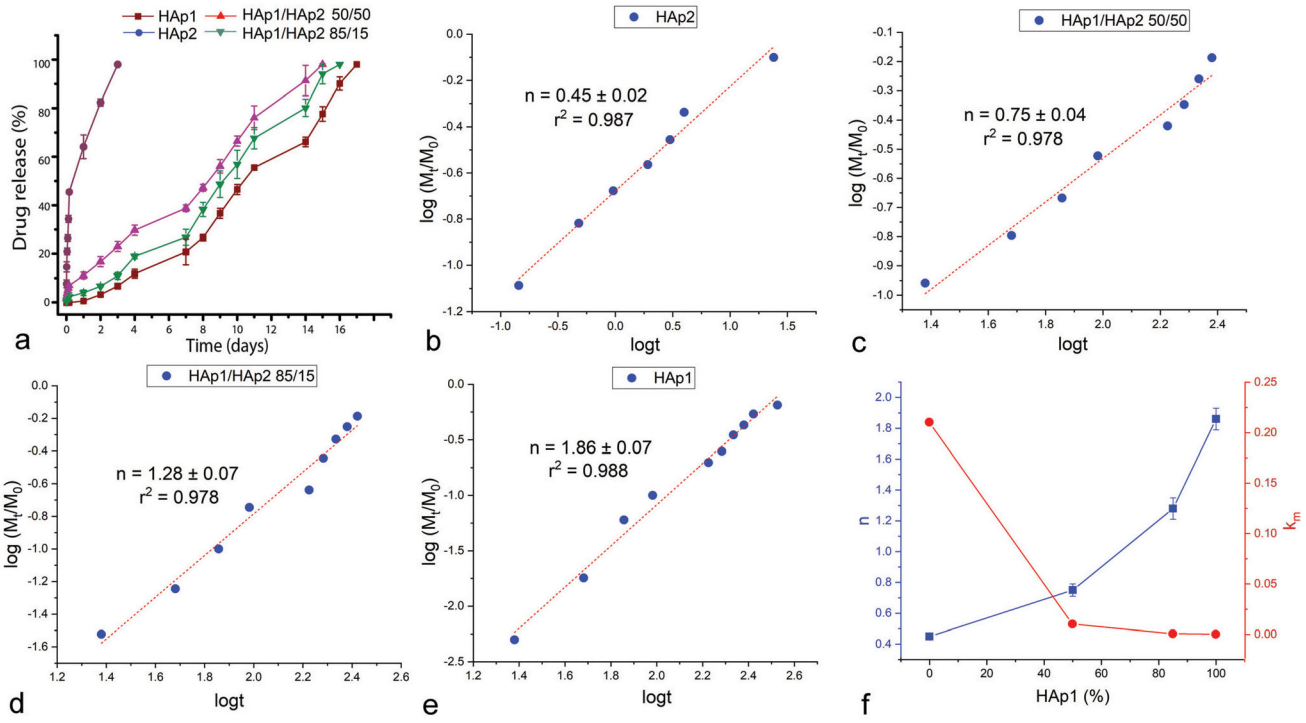

Fig. 4.

Ciprofloxacin kinetic release profiles of cements composed of HAp1 and HAp2 alone and HAp1 and HAp2 mixed in 85/15 and 50/50 weight ratios (a). Linear fits of the release data for the four different cements, including HAp2 (b), HAp1/HAp2 50/50 (c), HAp1/HAp2 85/15 (d) and HAp1 (e), to the Korsmeyer–Peppas model, from which the Korsmeyer–Peppas exponent, n, was derived. Variation in the parameter n and the release rate constant, k_m, as a function of the content of HAp1 in the mixed cements (f).

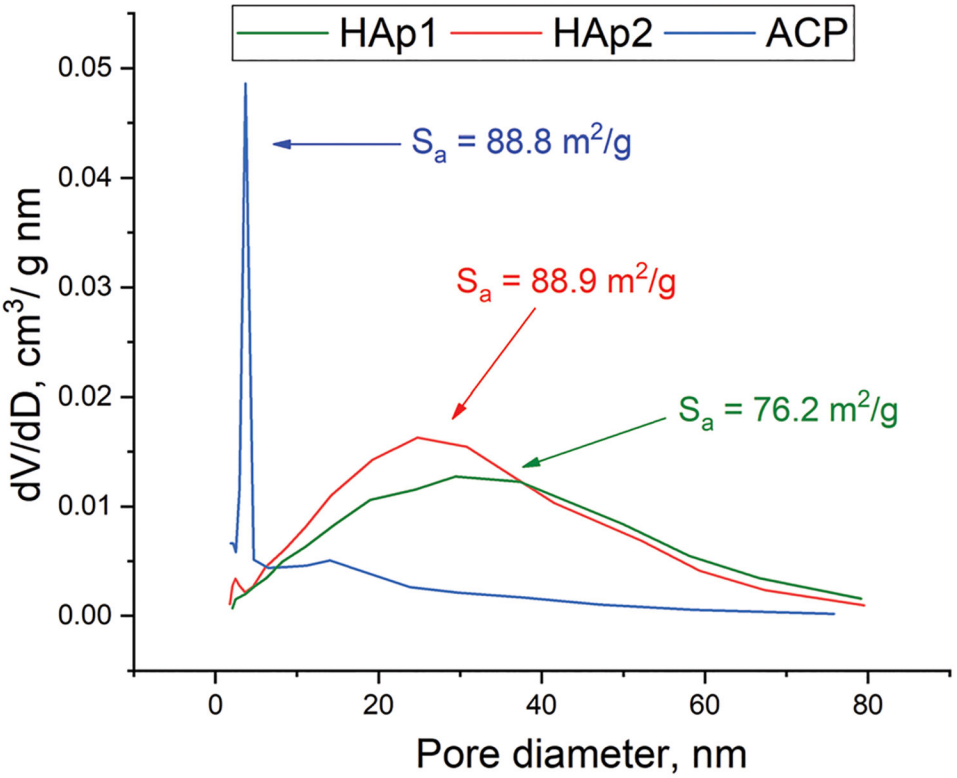

Fig. 5.
Cumulative pore size distributions and S_a values for HAp1, HAp2 and ACP.

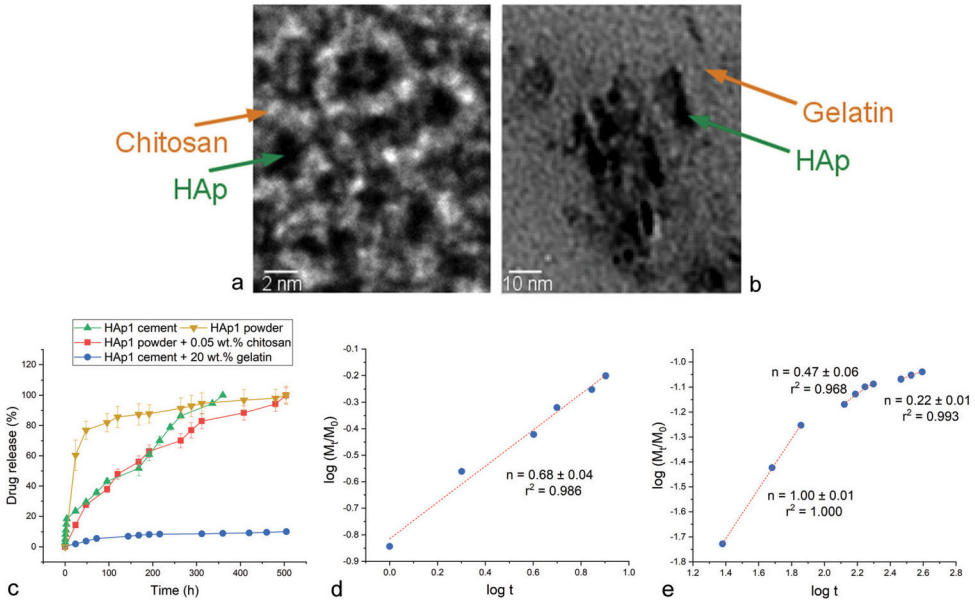

Fig. 6.

TEM images of HAp1 powder combined with 0.05 wt% chitosan (a) and of HAp1 cement combined with 20 wt% gelatin (b). Drug release profiles of HAp1 powder, HAp1 powder combined with 0.05 wt% chitosan, HAp1 cement and HAp1 cement combined with 20 wt% gelatin (c), along with the linear fits of the release from the HAp1 powder combined with 0.05 wt% chitosan (d) and from the HAp1 cement combined with 20 wt% gelatin (e) to the Korsmeyer–Peppas model, from which the Korsmeyer–Peppas exponent, *n*, was derived.

Table 1

Composition of the solid phase of the synthesized drug-loaded cement samples

Cement	HApl (g)	HAp2 (g)	Drug (g)
HApl	0.8	0	0.02
HAp1/HAp2 50/50	0.4	0.4	0.02
HAp1/HAp2 85/15	0.68	0.12	0.02
HAp2	0	0.8	0.02